

ϵ -near-zero (ENZ) graded index quasi-optical devices: steering and splitting millimeter waves

V. Pacheco-Peña,^{1,a)} V. Torres,^{1,b)} M. Beruete,^{1,c)} M. Navarro-Cía^{2,3,4,d)}
and Nader Engheta^{5,e)}

¹TERALAB (MmW—THz—IR & Plasmonics Laboratory), Universidad Pública de Navarra, Campus Arrosadía, 31006 Pamplona, Spain

²Optical and Semiconductor Devices Group, Department of Electrical and Electronic Engineering, Imperial College London, London SW7 2BT, UK

³Centre for Plasmonics and Metamaterials, Imperial College London, London SW7 2AZ, UK

⁴Centre for Terahertz Science and Engineering, Imperial College London, London SW7 2AZ, UK

⁵Department of Electrical and Systems Engineering, University of Pennsylvania, Philadelphia, PA 19104, USA.

Graded index ϵ near-zero (GRIN-ENZ) quasi-optical components such as beam steerers and power splitters are designed, simulated and analyzed.

The GRIN-ENZ medium is realized using stacked narrow hollow waveguides whose infinite array shows the first transmission peak at 1.0002 THz. Several GRIN-ENZ beam steerers to channel a normal incident plane wave to different output angles (15, 45, 65 and 80 deg) with good impedance matching (low reflection) are analytically and numerically demonstrated using planar structures with a thickness of $5\lambda_0 = 1500 \mu\text{m}$ along z -axis. Moreover, symmetrical and asymmetrical power splitters are designed with output angles (± 45 deg) and (-80, +35 deg), respectively.

^{a)} Electronic mail: victor.pacheco@unavarra.es

^{b)} Electronic mail: victor.torres@unavarra.es

^{c)} Electronic mail: miguel.beruete@unavarra.es

^{d)} Electronic mail: m.navarro@imperial.ac.uk

^{e)} Electronic mail: engheta@ee.upenn.edu

Metamaterials have attracted the attention of the scientific community in the last years because they have opened the possibility to generate arbitrarily tailored electromagnetic (EM) parameters such as low (i.e., less than unity) or even negative [1,2] values of permittivity (ϵ) and permeability (μ). In the realm of metamaterials, artificial materials with ϵ near-zero (ENZ) are becoming a prominent subfield by their own merits. It was demonstrated in the past that narrow hollow waveguides working near their cut-off frequency can be used to emulate an effective ENZ medium exhibiting unconventional features such as tunneling, squeezing and supercoupling. [3–6] Moreover, ENZ metamaterials have been reported recently at near infrared and visible frequencies by using metal-dielectric-metal (MIM) multilayers. [7–10]

Lenses have benefited greatly from the concepts of artificial materials [1,2,11]. Negative refractive index metamaterial lenses [2,12–14] and lenses with both near-zero (NNZ) ϵ and μ values have been reported.[15] Also, ENZ lenses have been analyzed [16–18] and GRIN concepts have been applied to make them more compact.[19–22]

Quasi-optical elements such as steerers and power splitters are also technologically interesting. Recently, artificial devices able to deflect electromagnetic waves have been reported using transformation optics [23], metal-dielectric GRIN structures [24] and Luneburg lens concepts [25]. Nevertheless, ENZ concepts have not been exploited for them yet, despite the fact that they promise low insertion loss because of the minimization of the impedance mismatch.

In this paper, GRIN-ENZ beam-steerers and power-splitters are designed, simulated and analyzed by simply stacking narrow hollow rectangular waveguides. To begin with, a beam-steerer structure with a cut of 45 degrees at its output (i.e. a prism), is studied in order to show its behavior using an array of identical waveguides. This structure is compared with an ideal homogeneous isotropic medium with refractive index near zero, demonstrating that homogenization holds for this type of structures. The study continues with GRIN-ENZ: Plano-planar beam-steerers and power splitters. By engineering the hollow dimensions of each waveguide, the beam-steerers are designed to deflect an incoming normal incident plane wave to different output angles (15, 45, 65 and 80 deg). Additionally, the power splitter is designed in order to obtain symmetrical (± 45 deg) and asymmetrical (-80, +35 deg) output angles.

A way to emulate the EM response of artificial structures such as metamaterials is by using the

intrinsic structural dispersion of a waveguide. In fact, in 1962 W. Rotman used this approach to emulate plasmas at microwave frequencies [26] using parallel-plate waveguides. It is important to highlight that, strictly speaking, an array of waveguides cannot be described by a dielectric function because it is not a continuous medium. However, as it will be described next, the EM response of this waveguide array can be approximated using a Drude model, which at a particular frequency, has ENZ characteristic. Its frequency response can be engineered by varying its dimensions. Finally, it is worth noting that the resulting equivalent medium is anisotropic, with ENZ response only for ϵ_{xx} but not for ϵ_{yy} and ϵ_{zz} at the operation frequency. In the following, we will refer only to ϵ_{xx} when we mention the relative effective permittivity ($\epsilon_{r_eff} = \epsilon_{xx}$), for clarity.

Let us consider a rectangular waveguide with its largest hollow dimension parallel to y-axis with metal dimensions d_x and d_y and hollow dimensions h_x and h_y [see figure 1 (right-bottom inset)]. By using a horizontally polarized E_x -wave, it is well known that the propagation constant (β) of its dominant mode (TE_{01}) can be calculated as follows [27]:

$$\beta = k_0 \sqrt{1 - \left(\frac{\pi}{k_0 h_y} \right)^2} = \frac{2\pi}{\lambda_{wg}} \quad (1)$$

where k_0 is the wave number in the medium filling the waveguide at the working frequency (f) calculated as $k_0 = 2\pi f/c$, λ_{wg} is the guided wavelength and c is the velocity of light in the filling medium, which in our case is vacuum. This expression shows that the frequency response of a rectangular waveguide is intrinsically dispersive. This property permits to have a wide variety of electromagnetic responses when a medium is synthesized using an array of waveguides. Such homogenized medium can be considered equivalent to a metamaterial with dispersive relative effective permittivity (ϵ_{r_eff}) [6]. In fact, it has been reported that, a rectangular waveguide working near cut-off mimics an ENZ metamaterial, since the propagation constant is lower than the wave number (k_0), [5] i.e., the guided wavelength is much larger than the free-space wavelength ($\lambda_{wg} \gg \lambda_0$). Based on this, and considering the rectangular waveguide as an effective medium, the relative effective permittivity can be calculated as follows [17]:

$$\epsilon_{r_eff} = 1 - \left(\frac{\pi}{k_0 h_y} \right)^2 \quad (2)$$

where $\mu_{r_eff} = 1$ is assumed considering that the equivalent medium only has electric response. Note that, when the h_y dimension is $h_y \rightarrow \lambda_0/2$ (i.e. the waveguide approaches cutoff) the waveguide models a

medium where $k = \beta \rightarrow 0$, with zero permittivity and zero phase variation (ψ), and an infinite wavelength (λ_{wg}) inside the waveguide. It is worth remarking that the relative effective permittivity $\epsilon_{r_eff} = 0$ is an ideal case and in practice it cannot be exactly reached due to the absorption inside the waveguide. Therefore the operational frequency will be near, but not exactly at, the cut-off frequency.

Based on this, let us study the rectangular narrow hollow waveguide shown in figure 1, which will be used as reference in the design of the GRIN-ENZ beam steerers and power splitters. In order to show its behavior, the dimension h_y is fixed to work near the cutoff wavelength of the fundamental mode for a rectangular waveguide TE_{01} : $h_y \approx \lambda_0/2$, where λ_0 is the free-space wavelength; at the operation frequency of 1 THz, $\lambda_0 = 300 \mu\text{m}$. Moreover, it has been demonstrated in [3,17] that by reducing h_x drastically, impedance matching with free space can be achieved along with the ENZ property. Based on this, the narrow dimension (h_x) of the waveguide is chosen following the ratio $h_x/h_y = 0.04$.

With these considerations, the waveguide is simulated using the commercial software CST Microwave StudioTM with the design parameters: $l_z = 5\lambda_0 = 1500 \mu\text{m}$, $d_x = 60 \mu\text{m}$, $d_y = 200 \mu\text{m}$, $h_y = 150 \mu\text{m}$ and $h_x = 6 \mu\text{m}$. The incident wave is polarized along x , E_x , and propagates along z -axis. Accordingly, top and bottom magnetic walls and, electric walls are used at the left and right side of the unit cell in order to imitate an infinite waveguide array along both transversal directions. Moreover, an electric field probe is placed at ($x = y = 0 \mu\text{m}$, $z = 1500 \mu\text{m}$), i.e., just at the output of the rectangular waveguide, in order to record the waveforms at this position and obtain the corresponding spectra by Fourier transformation.

Simulation results of the normalized E_x -field magnitude for the frequency range 0.97-1.01 THz are presented in figure 1. The maximum transmission appears at $f_0 = 1.0002$ THz (above and near cut-off). At this frequency, the propagation constant for the narrow hollow waveguide is $\beta_0 = \psi/l_z = 1.22 \text{ rad}/1500 \mu\text{m} = 813.33 \text{ rad/m}$, much smaller than the wavenumber in free-space ($k_0 = 20948.14 \text{ rad/m}$). With this value of β_0 and using (2), the relative effective permittivity obtained is $\epsilon_{r_eff} = 0.0015$, confirming that the effective permittivity is actually near zero (ENZ) and the waveguide mimics an ENZ medium at the fundamental band [3]. The tunneling effect at this frequency can be observed in figure 1 (left inset) where simulation results of the E_x -magnitude and H_y -phase are presented [inset (a) and (c), respectively]. The uniform E -field distribution with the small phase variation observed for the H -field corroborate the ENZ behavior. It is important to highlight that another transmission peak appears at 1.0061 THz which corresponds to a half-wavelength Fabry-Perot (FP) resonance. [5] The Fabry-Perot

nature of this higher band can be easily unveiled from the same kind of E_x -magnitude and H_y -phase plots [see inset (b) and (d), respectively]. It can be observed that the field is no longer uniform inside the waveguide and the H_y -phase suffers more variation (~ 160 deg) compared with the tunneling ENZ frequency band.

It is known that EM waves emerging from an ENZ medium propagate perpendicular to its surface, i.e., they follow the shape of the output face due to the nearly uniform phase progression inside the medium [16,28]. Applying this property, a beam-steerer (i.e. a prism) is designed and simulated in order to show that it is possible to change the direction of an incoming plane wave to any output angle (45 deg in our design) by simply stacking waveguides of different length (l_z). The structure is shown in figure 2 (b) and consists of 37 waveguides with the same transversal dimensions as the unit cell described before (see bottom-right inset in figure 1) and a length l_z which varies from 280 μm to 2500 μm . Since the electric field lies on the xz -plane, the structure is infinitely replicated along y -axis by imposing top and bottom magnetic walls. Moreover, open boundaries (i.e. perfectly matched layers) are selected for the other planes and perfect electric conductor (PEC) is chosen for the prism material. Simulation results of the H_y -field at the ENZ frequency ($f = 1.0002$ THz) are presented in figure 2 (b). It can be observed that the wavefront actually follows the inclination of the output face. In order to compare this structure with the ideal case, simulation results of the H_y -field distribution of an isotropic homogeneous zero refractive index slab ($\epsilon = \mu = n \approx 0$) is shown in figure 2 (a). The performance of both structures is almost identical, demonstrating that our prism emulates an ENZ medium.

A major drawback of this design is its relatively large volume which can be reduced using GRIN-ENZ structure [17,29] i.e., a beam steerer with parallel faces or uniform length (l_z), where the refractive index of each waveguide is changed by simply tuning their hollow dimensions so that the phase at the output is gradually modulated. Thus, each waveguide must be tuned to give a particular phase delay at the output. This phase delay depends on the operational frequency, waveguide location and the phase delay inside a reference waveguide. The behavior of the beam steerer can be easily obtained from ray tracing assuming that the slab is discretized in $m+1$ waveguides with a periodicity d_x . This is schematically shown in figure 2(c), where md_x is the distance between the reference waveguide (right most waveguide) and each one of the other array elements, and d_i is the excess distance travelled by the wave emitted by each waveguide with respect to the reference. With these considerations, we end up with the following equation:

$$\Delta\psi^{(m)} = \beta^{(m)}l_z = \beta_0l_z - k_0(md_x)\sin(\theta) + 2\pi n \quad (3)$$

where l_z is the thickness of the slab, k_0 is the wave number in free space, β_0 is the propagation constant of the guided mode of the rightmost waveguide used as reference, m is an integer number $m=1,2,3,\dots$ which represents the waveguide number, $\Delta\psi^{(m)}$ is the phase delay difference between the m th waveguide and the reference one, $\beta^{(m)}$ the propagation constant at the position md_x , and n is an integer number $n=1,2,3,\dots$ which represents a phase change of $2\pi n$. Moreover, by using (1) it is straightforward to fulfill equation (3) by tuning the height of each hollow $h_y^{(m)}$. So far the design enforces certain $h_y^{(m)}$ for each waveguide; however, $h_x^{(m)}$, the width of each hollow, is still a free parameter that can be used to impedance match each waveguide to free-space [4,17] and minimize Fresnel reflection losses of the overall graded index lens. The free-space matching is achieved by imposing:

$$h_x^{(m)} = \frac{h_y^{(m)}d_x\beta^{(m)}}{k_0d_y} \quad (4)$$

Based on this, the GRIN-ENZ Beam steerer is designed to work at $f \sim 1$ THz ($\lambda \sim 300 \mu\text{m}$) with the following dimensions: thickness $l_z = 5\lambda_0 = 1500 \mu\text{m}$, total width $10\lambda_0$ (which means $m+1 = 50$ waveguides) and $\theta = 45^\circ$, see figure 2(c-d). The $h_y^{(m)}$ and $h_x^{(m)}$ dimensions of each waveguide are straightforwardly computed using (1),(3-4). For the numerical analysis, the finite-integration software CST Microwave Studio™ is used applying the same boundary conditions as the previous prism; i.e., top and bottom magnetic walls and open boundary conditions on the right- and left-hand side of the simulation box. Also perfect electric conductor (PEC) is chosen for the steerer. The designed structure is shown in figure 2(d).

Simulation results showing the H_y -field distribution are presented in figure 2(f) and compared with analytical calculations considering Huygens-Fresnel approximation of isotropic point sources placed at each waveguide output position, with unit amplitude and phase calculated as:

$$\phi^{(m)} = k_0\sqrt{\epsilon_{r_eff}^{(m)}}l_z \quad (5)$$

that emit a cylindrical wave, figure 2(e). Using this principle, we calculate the angular distribution of the power at a distance r for angles from 0 to +90 deg. The value of r has been selected to be $100 \text{ mm} = 333.33\lambda_0$ in order to calculate the output angle far away from the steerer [see bottom panel of figure 2(e)].The results obtained demonstrate that both structures allow deflecting the incoming 0 deg plane

wave to an output angle of 45 deg. Moreover, from figure 2(f), it can be seen that the wave front at the output has a better quality than the one observed with the prism in figure 2(b) because the edge diffraction has been minimized by placing more metal on both sides of the lens, as shown in figure 2(d).

A standing wave at the input of the beam steerer reveals some impedance mismatch. The design is done using the local periodicity approximation, where each waveguide parameters are obtained assuming an infinite array of identical waveguides. Hence, the final design is not perfectly matched to free-space. [17] The reflection coefficient ($|\Gamma|$) can be calculated as $(A_{max}/A_{min}) = (1+|\Gamma|)/(1-|\Gamma|)$ where A_{max} and A_{min} are the maximum and minimum values of the field magnitude; the approximate value obtained is $|\Gamma| = -7.2\text{dB}$ which represents a moderately good impedance matching. For the sake of comparison, a common millimeter-wave dielectric quasi-optical element made of silicon, with relative permittivity $\epsilon_r = 11.9$, has $|\Gamma| \sim -5.5$ to -5.19 dB. [30,31]

Applying similar principles, GRIN-ENZ beam steerers are designed and simulated for output angles of 15, 65 and 80 deg. Simulation results are presented in figure 3. At the right side of each structure, the phase delay difference introduced for each waveguide along with the relative effective permittivity calculated from (2) are plotted. It is clear that the output angle for each structure is in good agreement with the designed value. Moreover, it can be observed that the value of ϵ_{r_eff} is close to 0 (maximum = 0.16) for each individual waveguide of all the structures. The reflection coefficient is -9.5 dB, -6 dB and -5.8 dB for the output angle of 15 deg, 65 deg and 80 deg, respectively. Note that the minimum $|\Gamma|$ is obtained for the 15 deg design. This result can be explained as follows: for small output angles the phase difference between waveguides and, therefore the difference in their dimensions [see Eqs. (1), (3) and (4)] is less than for larger angles. Then, our design which is based on the local periodicity approximation (i.e. the design of each waveguide is done assuming an infinite array of identical waveguides) is better suited for small angles.

Next, several GRIN-ENZ power splitters are demonstrated, able to deflect a normally incident wave in two waves with different angles at the output. The designs consist of 100 waveguides with a total width of $20\lambda_0$. To get the double angle operation, two waveguides with the dimensions shown in figure 1(b) are used as reference. They are placed at the extremes of the whole structure (one at the left and one at the right). Note that a straight way to design a power splitter with symmetrical output angles is by joining together side by side two of the blocks shown previously. By using (1),(3-4), two power

splitters are designed: a structure with symmetric output angles (± 45 deg) and one with different angles at its output (-80 deg and $+35$ deg). The hollow dimensions ($h_y^{(m)}$ and $h_x^{(m)}$) for each waveguide are shown in figure 4(a,b) for the first and second design, respectively. Moreover, the phase delay difference along with the relative effective permittivity calculated from (2) for each waveguide are plotted in figure 4(c,d) for output angles of ± 45 deg and $(-80, +35)$ deg, respectively. Simulation results of the power distribution in xz -plane are presented in figure 4(f,h) for both designs, respectively. As can be observed, the output angles are in good agreement with the designed values. Also, as it was done with the beam steerer for an output angle of 45 deg, the analytical study of both power splitters using the Huygens-Fresnel principle is presented in figure 4(e,g) along with the normalized power distribution calculated for angles from -90 to 90 deg at the distance $r = 100$ mm $= 333.33\lambda_0$ in order to better compare the contribution of both output angles of each beam splitter [see bottom panel of figure 4(e,g)]. It can be observed that analytical and numerical results are in good agreement, validating both designs. Moreover, the reflection coefficient is -7.13 dB and -6.55 dB for the symmetric and asymmetric beam splitters, respectively, demonstrating the beam splitting capability of these structures.

In conclusion, different ENZ structures have been designed and numerically simulated using stacked narrow hollow rectangular waveguides. The ENZ performance of the unit cell has been presented, demonstrating two peaks of high transmission: one related to the tunneling frequency (ENZ behavior) and another due to a half-wavelength FP resonance. Moreover, different designs of GRIN ENZ beam steerers with output angles of 15 , 45 , 65 and 80 degrees have been presented with a maximum and minimum value of reflection coefficient $|\Gamma|$ of -5.8 dB and -9.5 dB for the designs at 80 deg and 15 deg respectively. Also, symmetrical and asymmetrical double angle GRIN ENZ power splitters have been reported, demonstrating the good agreement between simulation and the designed output angles. Results presented here could find applications in novel beam shapers and launchers of surface waves.

ACKNOWLEDGMENTS

This work was supported in part by the Spanish Government under contract Consolider Engineering Metamaterials CSD2008-00066 and contract TEC2011-28664-C02-01. V.P.-P. is sponsored by Spanish Ministerio de Educación, Cultura y Deporte under grant FPU AP-2012-3796. V.T. is sponsored by the Universidad Pública de Navarra. M.B. is sponsored by the Spanish Government via RYC-2011-08221. M. N.-C. is supported by the Imperial College Junior Research

Fellowship. In memoriam of our beloved friend Mario Sorolla.

REFERENCES

- [1] Engheta N and Ziolkowski R 2006 *Metamaterials: Physics and Engineering Explorations* (USA: John Wiley & Sons & IEEE Press)
- [2] Pendry J B 2000 Negative refraction makes a perfect lens *Phys. Rev. Lett.* **85** 3966–9
- [3] Silveirinha M and Engheta N 2006 Tunneling of Electromagnetic Energy through Subwavelength Channels and Bends using ϵ -Near-Zero Materials *Phys. Rev. Lett.* **97** 157403–1–4
- [4] Silveirinha M G and Engheta N 2007 Theory of supercoupling , squeezing wave energy , and field confinement in narrow channels and tight bends using ϵ -near-zero metamaterials **76** 245109–1–17
- [5] Alù A, G. Silveririnha M and Engheta N 2008 Transmission-line analysis of ϵ -near-zero – filled narrow channels *Phys. Rev. E* **78** 016604–1–10
- [6] Edwards B, Alù A, Young M, Silveirinha M and Engheta N 2008 Experimental Verification of Epsilon-Near-Zero Metamaterial Coupling and Energy Squeezing Using a Microwave Waveguide *Phys. Rev. Lett.* **100** 033903
- [7] Subramania G, Fischer a. J and Luk T S 2012 Optical properties of metal-dielectric based epsilon near zero metamaterials *Appl. Phys. Lett.* **101** 241107
- [8] Zhang S, Fan W, Panoiu N C, Malloy K J, Osgood R M and Brueck S R J 2005 Experimental demonstration of near-infrared negative-index metamaterials *Phys. Rev. Lett.* **95** 137404–1–4
- [9] Maas R, Parsons J, Engheta N and Polman A 2013 Experimental realization of an epsilon-near-zero metamaterial at visible wavelengths *Nat. Photonics* **7** 907–12
- [10] Gao J, Sun L, Deng H, Mathai C J, Gangopadhyay S and Yang X 2013 Experimental realization of epsilon-near-zero metamaterial slabs with metal-dielectric multilayers *Appl. Phys. Lett.* **103** 051111
- [11] Veselago V G 1968 The electrodynamics of substances with simultaneously negative values of ϵ and μ *Sov. Phys. Uspekhi* **10** 509–14
- [12] Beruete M, Navarro-Cía M, Sorolla M and Campillo I 2008 Planoconcave lens by negative refraction of stacked subwavelength hole arrays *Opt. Express* **16** 9677–83
- [13] - , Beruete M, Sorolla M and Campillo I 2009 Converging biconcave metallic lens by double-negative extraordinary transmission metamaterial *Appl. Phys. Lett.* **94** 144107
- [14] Parazzoli C G, Greigor R B, Nielsen J A, Thompson M A, Li K, Vetter A M, Tanielian M H and Vier D C 2004 Performance of a negative index of refraction lens *Appl. Phys. Lett.* **84** 3232–4
- [15] Navarro-Cía M, Beruete M, Campillo I and Sorolla M 2011 Enhanced lens by ϵ and μ near-zero metamaterial boosted by extraordinary optical transmission *Phys. Rev. B* **83** 115112–1–5
- [16] Navarro-Cía M, Beruete M, Sorolla M and Engheta N 2012 Lensing system and Fourier transformation using epsilon-near-zero metamaterials *Phys. Rev. B* **86** 165130–1–6
- [17] Torres V, Pacheco-Peña V, Rodríguez-Ulibarri P, Navarro-Cía M, Beruete M, Sorolla M and Engheta N 2013 Terahertz epsilon-near-zero graded-index lens *Opt. Express* **21** 9156–66

- [18] Torres V, Orazbayev B, Pacheco-Peña V, Beruete M, Navarro-Cía M and Engheta N 2014 Experimental demonstration of a millimeter-wave metallic ENZ lens based on the energy squeezing principle *IEEE Trans. Antennas Propag.* (Submitted)
- [19] Paul O, Reinhard B, Krolla B, Beigang R and Rahm M 2010 Gradient index metamaterial based on slot elements *Appl. Phys. Lett.* **96** 241110–1–3
- [20] Neu J, Krolla B, Paul O, Reinhard B, Beigang R and Rahm M 2010 Metamaterial-based gradient index lens with strong focusing in the THz frequency range *Opt. Express* **18** 27748–57
- [21] Liu R, Cheng Q, Chin J Y, Mock J J, Cui T J and Smith D R 2009 Broadband gradient index microwave quasi-optical elements based on non-resonant metamaterials **17** 21030–41
- [22] Driscoll T, Basov D N, Starr a. F, Rye P M, Nemat-Nasser S, Schurig D and Smith D R 2006 Free-space microwave focusing by a negative-index gradient lens *Appl. Phys. Lett.* **88** 081101
- [23] Kwon D-H and Werner D H 2009 Beam Scanning Using Flat Transformation Electromagnetic Focusing Lenses *IEEE Antennas Wirel. Propag. Lett.* **8** 1115–8
- [24] Lin X Q, Cui T J, Chin J Y, Yang X M, Cheng Q and Liu R 2008 Controlling electromagnetic waves using tunable gradient dielectric metamaterial lens *Appl. Phys. Lett.* **92** 131904
- [25] Demetriadou A and Hao Y 2011 A Grounded Slim Luneburg Lens Antenna Based on Transformation Electromagnetics *IEEE Antennas Wirel. Propag. Lett.* **10** 1590–3
- [26] Rotman W 1962 Plasma simulation by artificial dielectrics and parallel-plate media *IRE Trans. Antennas Propag.* **10** 82–95
- [27] Pozar D M 1998 *Microwave Engineering* (New York: John Wiley & Sons)
- [28] Alù A, Silveirinha M, Salandrino A and Engheta N 2007 Epsilon-near-zero metamaterials and electromagnetic sources: Tailoring the radiation phase pattern *Phys. Rev. B* **75** 155410
- [29] Smith D, Mock J, Starr a. and Schurig D 2005 Gradient index metamaterials *Phys. Rev. E* **71** 036609
- [30] Filipovic D F, Gearhart S S and Rebeiz G M 1993 Double-Slot Antennas on Extended Hemispherical and Elliptical Silicon Dielectric Lenses *IEEE Trans. Microw. Theory Tech.* **41** 1738–49
- [31] Raman S, Barker N S, Member S and Rebeiz G M 1998 A W -Band Dielectric-Lens-Based Integrated Monopulse Radar Receiver *IEEE Trans. Microw. Theory Tech.* **46** 2308–16

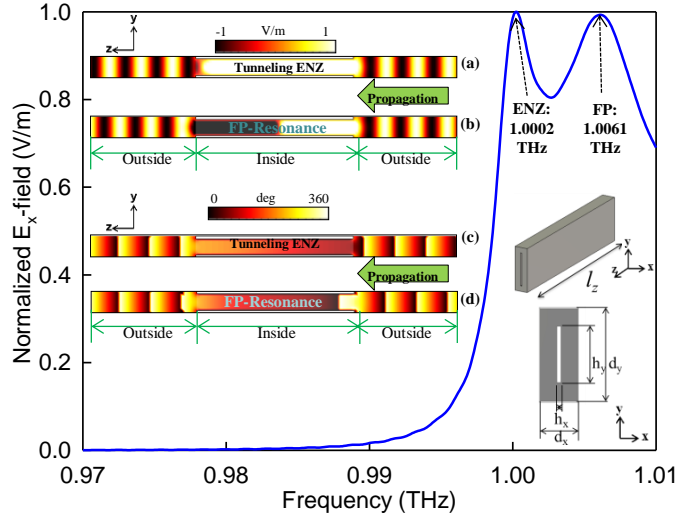


Figure 1. Simulation results of the normalized E_x -field magnitude (blue line) for the frequency range 0.97-1.01 THz. (Bottom-right inset) schematic representation, perspective and front view, of the narrow hollow rectangular waveguide with parameters: $d_x = 60 \mu\text{m}$, $d_y = 200 \mu\text{m}$, $h_x = 6 \mu\text{m}$, $h_y = 150 \mu\text{m}$ and $l_z = 1500 \mu\text{m}$. (Top-left inset) from top to bottom: simulation results of the E_x -field magnitude for the tunneling frequency (1.0002 THz) and Fabry-Perot resonance (1.0061 THz), and simulation results of the H_y -phase distribution for the tunneling frequency and FP resonance.

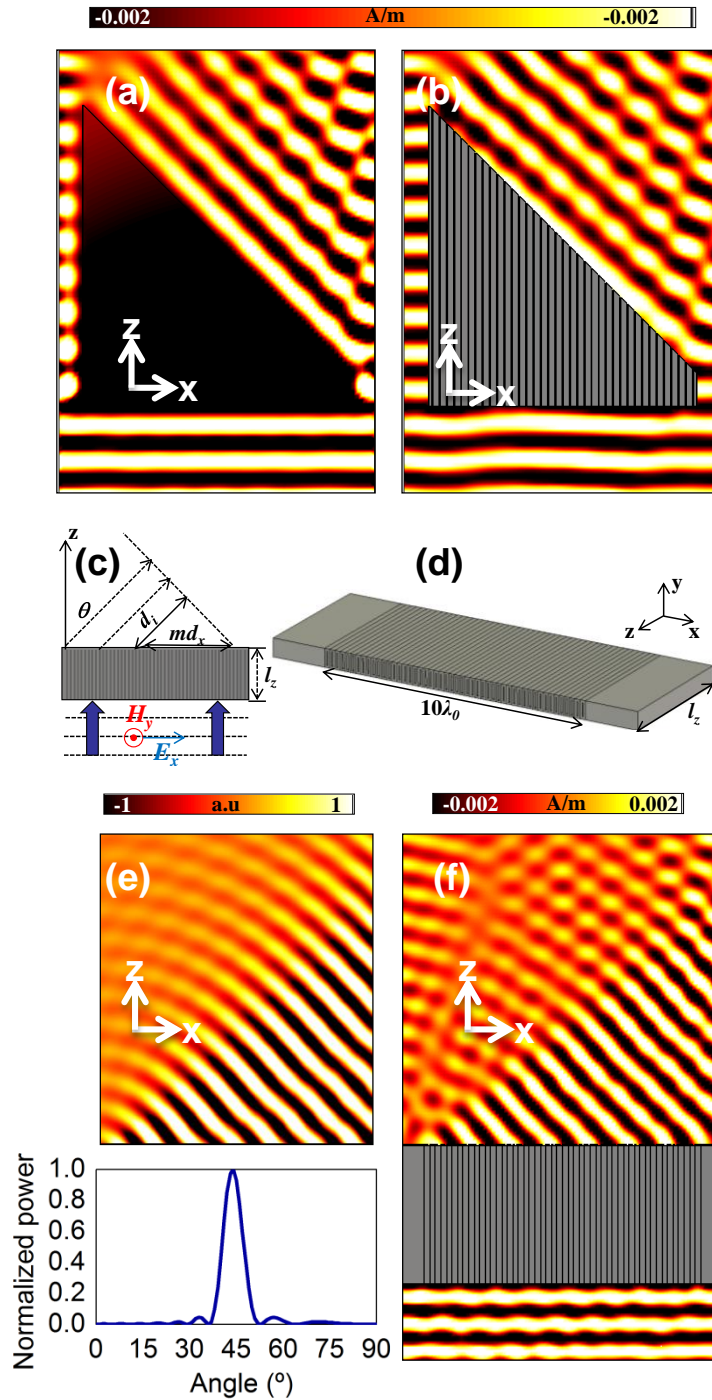


Figure 2. Simulation results of the H_y -field distribution of: (a) an isotropic homogeneous zero refractive index (impedance-matched) prism with its output face cut at 45 deg, and (b) an ENZ prism made with stacked narrow hollow rectangular waveguides with a cut of 45 deg at its output. (c) Geometrical representation of the graded index beam steering structure. (d) Designed GRIN ENZ structure for an output angle of 45 deg. (e) Analytical results of the field distribution using the Huygens-Fresnel principle in xz -plane along with the normalized power distribution at the fixed distance $r = 100$ mm from the steerer for angles from 0 to 90 deg in Cartesian coordinates (bottom panel). (f) Simulation results for the GRIN-ENZ beam steerer designed with stacked rectangular waveguides using CST Microwave StudioTM.

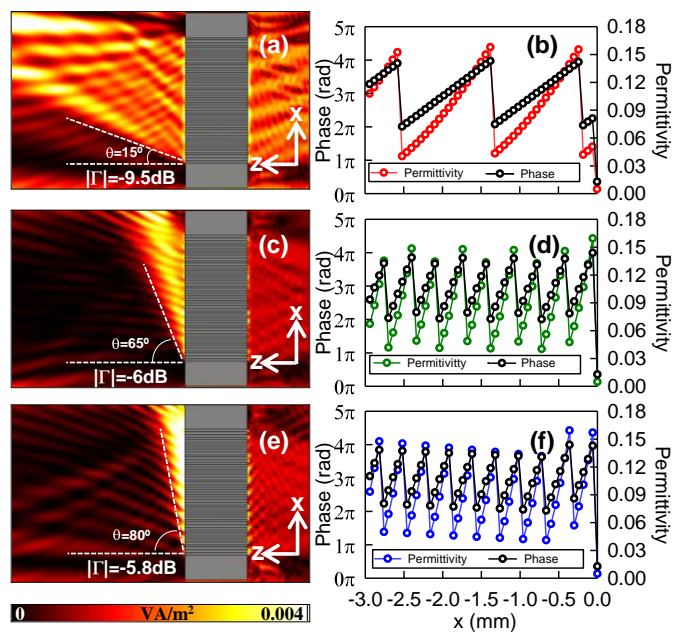


Figure 3. Spatial power distribution in xz - plane for the beam steerers designed for output angles of: (a) 15 deg, (c) 65 deg and (e) 80 deg. Phase progression allowed inside each waveguide along with the corresponding values of the relative effective permittivity for the beam steerers designed for output angles of: (b) 15 deg, (d) 65 deg and (f) 80 deg.

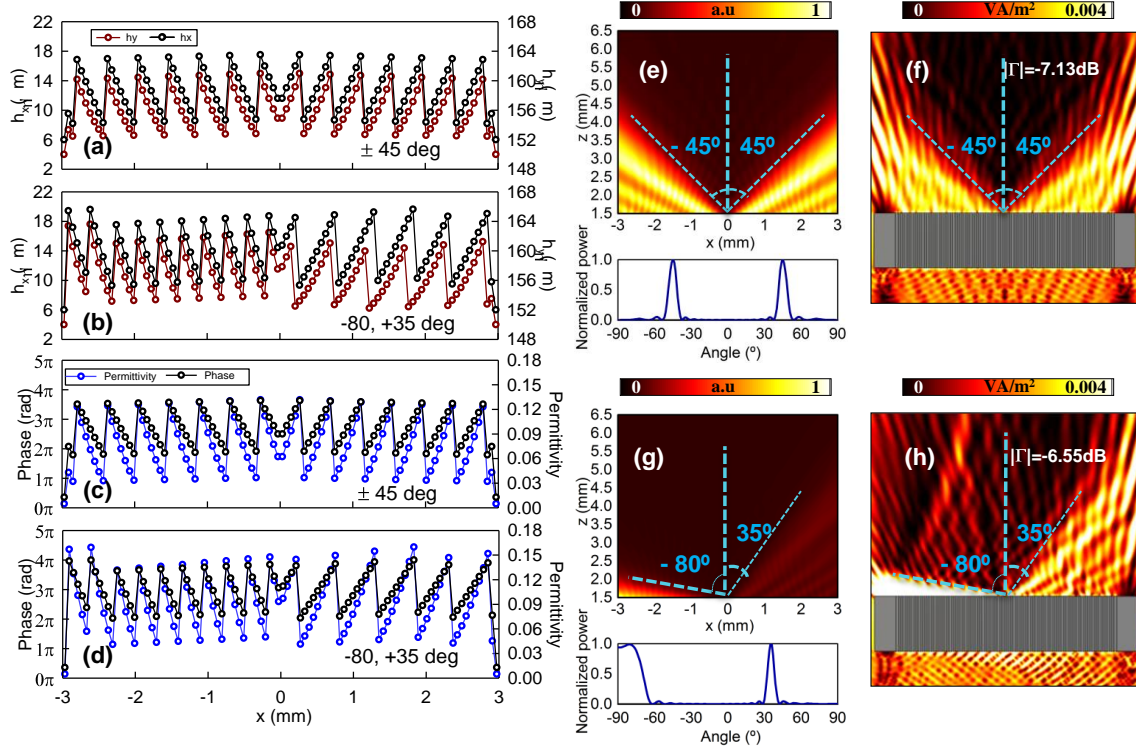


Figure 4. Hollow dimensions ($h_x^{(m)}$ and $h_y^{(m)}$) for each waveguide of the power splitters designed for output angles of (a) ± 45 degrees and (b) $-80, +35$ degrees. Phase progression allowed inside each waveguide along with the corresponding values of the relative effective permittivity for the power splitters designed for output angles of: (c) ± 45 degrees and (d) $-80, +35$ degrees. Analytical results of the spatial power distribution in xz - plane for: (e) a symmetric power splitter with output angle of ± 45 deg and (g) an asymmetric power splitter for -80 and $+35$ degrees as output angles. The bottom panel of these two figures is the normalized power distribution at the fixed distance $r = 100$ mm for angles from -90 to 90 deg calculated analytically. Simulation results of the spatial power distribution in xz - plane for: (f) a symmetric power splitter with output angle of ± 45 deg and (h) an asymmetric power splitter for -80 and $+35$ degrees as output angles.